On the effect of time lags on a saddle-node remnant in hyperbolic replicators

Joan Gimeno[1,2], Àngel Jorba[1,2] and Josep Sardanyés[3,2]

May 2018

(1) Departament de Matemàtiques i Informàtica, Universitat de Barcelona

(2) Barcelona Graduate School of Mathematics (BGSMath)

(3) Centre de Recerca Matemàtica (CRM)

Abstract

Saddle-node (s-n) bifurcations can be responsible for abrupt changes between alternative states in nonlinear dynamical systems. It is known that once a s-n bifurcation takes place, a s-n remnant (also named ghost or delayed transition) can continue attracting the flows in the phase space before they achieve another attractor. The time needed to pass through the saddle-remnant, which causes an extremely long transient after the bifurcation, is known to follow an inverse square-root law. In this manuscript we investigate the effect of time lags in the transient dynamics near a s-n bifurcation by means of delay differential equartions. To do so we use a one-variable dynamical system describing the dynamics of an autocatalytic replicator, introducing a time lag, τ, in the process of hyperbolic replication, becoming an ∞-dimensional dynamical system. We show that the delayed transitions found in the lagged system become much longer than the ones found in the system without time lags, although the inverse square-root law is preserved. The time the flows spend crossing the ghost is shown to increase linearly with τ. The implications of this transients' enlargement are discussed in the framework of prebiotic evolution.

Contents

1 Introduction

Bifurcations produce transitions separating different dynamical scenarios and can occur when one or more systems' parameters cross bifurcation values. The nature of the bifurcations can differ depending on the underlying nonlinear interactions found in a given dynamical system. Transitions between alternative states can be continuous or discontinuous (catastrophic) [1, 2]. For instance, smooth transitions such as second order phase transitions are typically given by transcritical bifurcations. This bifurcation involves the collision of fixed points and an exchange of stability between them [3].

A typical bifurcation giving place to catastrophic transitions (e.g. first-order phase transitions) is the saddle-node (hereafter s-n) bifurcation, studied in this article. This bifurcation involves the collision and annihilation of invariant objects such as fixed points [3] or periodic orbits [4, 5] (see [6] for evidences of a s-n of periodic orbits in experiments with a semiconductor laser with optical injection). S-n bifurcations arise in many biological dynamical systems with strong feedbacks such as cooperation [7] or facilitation processes in semiarid ecosystems [8], and factors such as mating or predation causing the so-called Allee effects [9], where the population size becomes crucial in the fate of the species. Also, catastrophic transitions have been discussed within the framework of ecosystems' dynamics under global change and anthropogenic pressure [1, 2, 8]. Interestingly, Dai et al. provided a detailed characterization of a s-n bifurcation obtained in experiments with yeast [10].

The dynamical behavior investigated in this article appears just after a s-n bifurcations and is given by the so-called *s-n remnant*, *bottleneck*, or *ghost* [3, 11]. This phenomenon involves a *delayed transition* required to pass through a bottleneck region where a s-n remnant continues influencing the flows after the collision of the saddle and the node [3]. Delayed transitions are also found in s-n bifurcations of periodic orbits [4, 5]. Indeed, experimental evidences in an electronic circuit suggests the presence of these long transients in oscillatory systems [12]. Also, slowing down phenomena due to a s-n bifurcation has been recently reported in asymmetric elastic 'snap-through' instabilities [13].

It is known that the slowing time, T, tied to s-n bifurcations typically follows an inverse square-root law, given by:

$$T \propto 1/\sqrt{\alpha - \alpha_c}, \tag{1}$$

α being the bifurcation parameter and α_c the bifurcation value at which the s-n bifurcation occurs. According to the normal form of s-n bifurcations in time continuous systems (flows), given by $\dot{x} = r + x^2$, we can consider that r is proportional to the distance from the bifurcation (occurring at $r = 0$), with $0 < r \ll 1$. To estimate the time spent in the bottleneck, T_d, the time taken for x to go from $-\infty$ to $+\infty$ can be computed by integrating x [3]:

$$\int_{-\infty}^{\infty} \frac{dx}{r + x^2} = \frac{\pi}{\sqrt{r}} = T_d.$$

The previous expression displays the generality of the inverse square-root law.

As mentioned, this power law has been characterized in an experiment with an electronic circuit modelling Duffing's equation [12]. Moreover, the inverse square-root law

has also been described in a mathematical model for charge density waves [11] as well as in catalytic networks with hypercycle architecture [14]. The ghost for hypercycles [7, 15, 16, 17] appears after a s-n bifurcation, as a result of the jump of the stable fixed point responsible of coexistence and the saddle to the complex phase space.

An important feature of many dynamical systems, especially those modeling physical or biological processes, is the presence of time lags. Time lags arise when the processes at a given time t depend on the processes that occurred in the past $(t-\tau)$, τ being the time lag. The impact of time lags in the dynamics of ordinary differential equations can be drastic since dimensionality becomes infinite once time lags are introduced, and even single variable, time-continuous systems can behave chaotically [18], a behavior restricted to $n \geq 3$-dimensional time-continuous dynamical systems without time delays [3].

Despite the impact of time lags in dynamics has been studied with diligence in biological [18, 19, 20], chemical [21, 22] and physical systems such as lasers (see [23] and references therein), their effects on transients near bifurcation thresholds remain unexplored. In this manuscript we investigate how the dynamics near a s-n remnant change due to time lags. To do so we use a simple dynamical model describing replicators' autocatalysis that suffer a s-n bifurcation. By autocatalysis we mean a species that reproduces hyperbolically at low population values, instead of exponentially. This type of reproduction, which involves the presence of s-n bifurcations under the processes of exponential decay and competition, has been used to study the population dynamics of cooperation [5, 7, 17, 24].

The paper is organized as follows. In Section 2 we introduce the autocatalytic replicator model. Subsection 2.1 provides a summary of the dynamics and the s-n bifurcation for this system given by a one-dimensional differential equation without time lags. Subsection 2.2 explores the impact of time lags after the s-n bifurcation by using a delay differential equation version of the autocatalytic replicator model. Finally, Section 3 is devoted to some conclusions.

2 Cooperative time-continuous model

In order to analyse the impact of the time lags in the transients tied to the saddle-node (s-n) remnant we analyze a simple one-dimensional continuous model suffering a s-n bifurcation. We focus on a model describing the dynamics of a single autocatalytic replicator [24, 16]. In Section A below we summarize the dynamics of the model with no time lags. Then, in Section 2.2 we will investigate how the dynamics near a s-n remnant vary by adding time lags.

2.1 Differential equation model without time lags

The model that we will here analyze describes the time dynamics of an autocatalytic replicator with intra-specific competition and density-independent degradation [24, 7]. The state variable $x(t)$ is the population of a replicator species that catalyzes its own replication. The dynamical system describing these process can be written as:

$$\frac{dx}{dt}(t) = f(x) = kx^2(t)\Big(1 - \frac{x(t)}{K}\Big) - \varepsilon x(t). \tag{2}$$

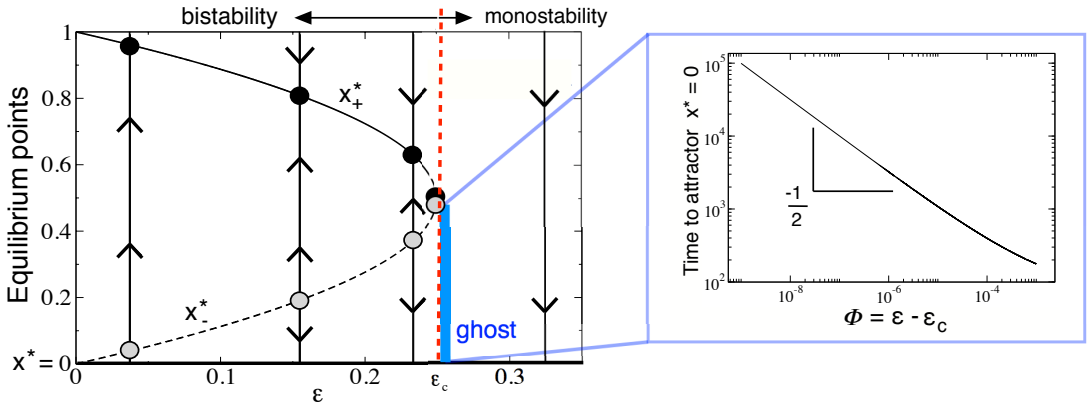

Figure 1: (Upper) Bifurcation diagram increasing the degradation rate, ε, for the autocatalytic replicator Eq. (2), using $k = 1$ (x^*_+ stable equilibrium (solid line); x^*_-: unstable (dashed line)). The arrows display the direction of the flows in the one-dimensional phase space, plotting x^*_+ (black circle) and x^*_- (gray circle). Notice that as $\varepsilon \to \varepsilon_c$ both equilibria collide in a saddle-node bifurcation (vertical red line). Just after the bifurcation the system experiences an extremely long transient towards the attracting fixed point $x^* = 0$ (small blue rectangle). Such a delayed transition follows the inverse square-root law as a function of the distance to the bifurcation value from above, $\Phi = \varepsilon - \varepsilon_c$, displayed at the panel below.

Parameters $k > 0$ and $\varepsilon > 0$ are the catalytic amplification rate and the degradation rate, respectively. The growth of the population is limited with a logistic function that introduced intra-specific competition, K being the carrying capacity (hereafter we consider $K = 1$). As previously mentioned, the replication term is non-linear (i.e., of the form kx^2) since there exists a density-dependent effect in the growth rate due to autocatalysis. An autocatalytic replicator, as a difference from a Malthusian one (which is amplified exponentially at low population numbers) follows the so-called hyperbolic growth. This growth involves that, for low population sizes (i.e., assuming $x(t)/K \approx 0$ and $\varepsilon = 0$), the population grows following $\dot{x} = kx^2$, with solution

$$x(t) = \frac{x(0)}{1 - x(0)kt}.$$

Note this type of replicators undergo explosive growth that can reach infinite populations at finite times. In our model we also consider density-independent degradation rate, given by constant ε, which is a necessary parameter to have a saddle-node (s-n) bifurcation.

Equation (2) has three equilibrium points $x_* \in \{x_0, x_\pm\}$, given by

$$x_0 = 0, \quad x_\pm = \frac{1}{2}\big(1 \pm \sqrt{1 - 4\varepsilon/k}\big). \tag{3}$$

Note that the pair $x_\pm$ will be biologically meaningful whenever $\varepsilon/k \leq 1/4$. Indeed, when $1 - 4\varepsilon/k = 0$ both fixed points x_+ and x_- have the same value, meaning that they collide. Such a collision leads to a s-n bifurcation occurring at the bifurcation value $\varepsilon_c = k/4$.

The stability of the fixed points can be obtained from the sign of $\lambda(x_*)$, with:

$$\lambda(x_*) = \frac{df}{dx}(x_*) = kx_*(2 - 3x_*) - \varepsilon.$$

From the previous expression we obtain that the fixed point $x_0 = 0$ is asymptotically locally stable since $\lambda(x_0) = -\varepsilon$, with $\varepsilon > 0$. We note that after the s-n bifurcation this fixed point becomes asymptotically globally stable. Further calculations allow us to obtain the following values for $\lambda(x_\pm)$:

$$\lambda(x_\pm) = 2\varepsilon - kx_\pm.$$

In particular, if $0 < \varepsilon/k < 1/4$, then x_+ is stable and x_- is unstable. As mentioned, for $\varepsilon > \varepsilon_c$ the fixed points $x_+, x_- \in \mathbb{C}$, being the point $x_0 = 0$ the only equilibrium in phase space, which is asymptotically globally stable.

The previous results on stability and existence of fixed points are displayed in Fig. 1, where the bifurcation diagram increasing ε is shown. Note that the two fixed points $x_\pm$ approach each other as ε increases, colliding at the bifurcation value (vertical red line). Just after the s-n bifurcation takes place, a s-n remnant appears and continues influencing the flows, and the transient times towards the global attractor x_0 become extremely long. The times of these transients have been computed numerically, and are displayed in the blue-framed panel of Fig. 1 at increasing ε above its bifurcation value. Note that this time follows the inverse square-root law, as mentioned in the Introduction. In the next Section we explore how time lags affect to the dynamics of the s-n remnant.

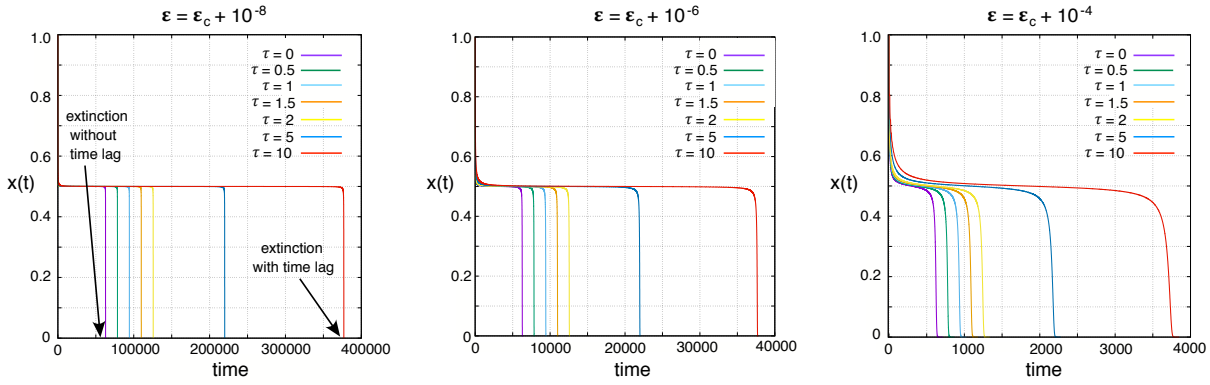

Figure 2: Extinction times near the saddle-node remnant for different time lags, τ, using $x(0) = 1$ as initial condition. The transients towards extinction have been computed for three different parameter distances to the bifurcation value ε_c for Eq. (4), with: $\varepsilon = \varepsilon_c + 10^{-8}$ (left panel); $\varepsilon = \varepsilon_c + 10^{-6}$ (middle); and $\varepsilon = \varepsilon_c + 10^{-4}$ (right panel). The violet trajectory in each panel corresponds to the case with no time lags. Notice that the increase of τ involves much longer transients.

2.2 Delay differential equation model

To investigate the impact of time lags in delayed transitions due to a saddle-node (s-n) remnant we here extend the model given by Eq. (2) to a delay differential equation (DDE)

including a time lag $\tau > 0$. The lagged model is given by:

$$\frac{dx}{dt}(t) = kx^2(t-\tau)\left(1 - \frac{x(t)}{K}\right) - \varepsilon x(t), \tag{4}$$

also setting $K = 1$. This model describes, in its simplest form, density-dependent reproduction of a single species with time lags. For instance, this model could be applied to autocatalytic molecules that spend some time in adopting the three-dimensional configuration necessary for providing catalysis, which could be delayed due to environmental conditions such as pH or temperature [25]. Other interpretations could consider the dynamics of a single species in which simultaneous hermaphroditism occurs and the individuals undergo a maturation time before reproduction. Hermaphroditism enables a form of sexual reproduction in which each partner can act as the "female" or the "male". Examples of simultaneous hermaphroditism, in which both male and female sexual organs are found in individuals at the same time, are found in gastropods, slugs, earthworms, nematodes, among others [26]. Indeed, a rough estimate of hermaphroditic animal species is 65,000 [27].

The main properties of the new model are summarized in the following statement:

Proposition 1 *The constant functions x_0 and $x_\pm$ defined in Eq. (3) are the only equilibrium points of Eq. (4) whose stabilities are independent of the delay τ. For $0 < \varepsilon/k < 1/4$, x_0 is exponentially stable, x_+ is stable and x_- is unstable, due to a real eigenvalue. At $\varepsilon/k = 1/4$ the equilibria x_- and x_+ merge at $x = 1/2$ in a s-n bifurcation and become complex for $\varepsilon/k > 1/4$.*

Proof. The equilibrium points are the constants functions that are roots of the right hand side of Eq. (4). That is, the same points x_* discussed in the previous Section, but its stability must be analyzed studying the transcendental eigenvalue problem for λ [28],

$$-kx_*^2 - \varepsilon + 2k(1-x_*)x_* e^{-\lambda\tau} - \lambda = 0,$$

which is equivalent to

$$(-kx_*^2 - \varepsilon)\tau e^{\lambda\tau} + 2k(1-x_*)x_*\tau - \lambda\tau e^{\lambda\tau} = 0. \tag{5}$$

Defining the values $p = (-kx_*^2 - \varepsilon)\tau$, $q = 2k(1-x_*)x_*\tau$, and $z = \lambda\tau$, then the Theorem 1 in [29] says that if $0 < \varepsilon/k < 1/4$ the stability of x_0 is subjected to the conditions $-\varepsilon < \min\{1/\tau, 0\}$ and $0 < ((\tan a_1)^2 + 1)^{1/2}$ while the stability of $x_\pm$ is subjected to $-kx_\pm < \min\{1/\tau, -2\varepsilon\}$ and $-2\varepsilon < ((a_1/\tau)^2 + (kx_\pm)^2)^{1/2}$ where in these conditions a_1 denotes the root of $a = p\tan a$ such that $0 < a < \pi$.

In particular, the stability of the real point x_* does not depend on the delay $\tau > 0$ and the conditions of being stable or unstable are the same as for the model without time lags. That is, $x_0 = 0$ is exponentially stable if and only if $-\varepsilon < 0$, and $x_\pm$ is exponentially stable if and only if $2\varepsilon - kx_\pm < 0$.

We have only shown whether the equilibrium points $x_0, x_\pm$ are stable or not but we did not quantify their stability. However, we can apply Lemma 1 in [29] to transform

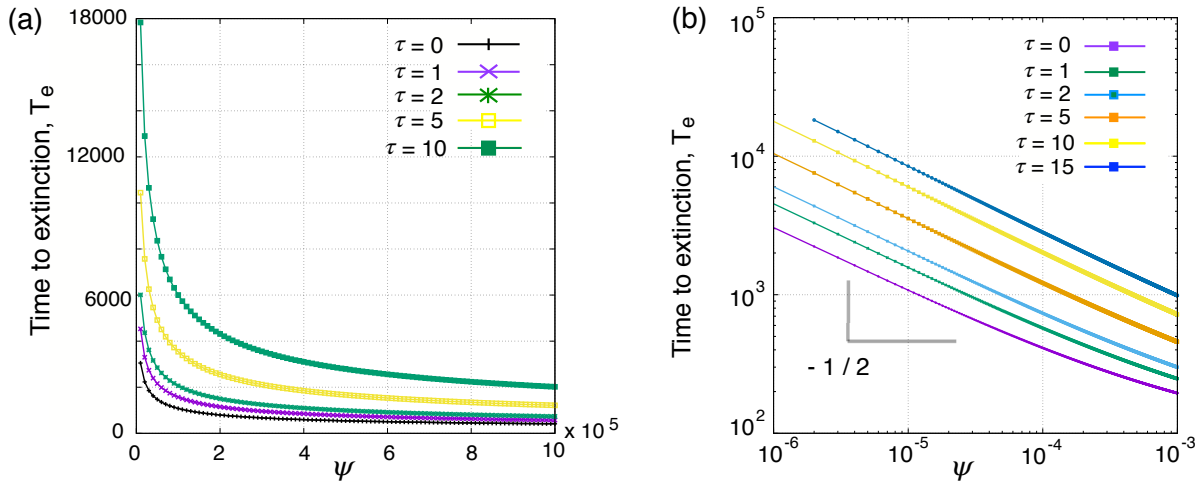

Figure 3: Dependence of extinction times (T_e) on the distance to bifurcation threshold, $\psi = \varepsilon - \varepsilon_c$. (a) Time to extinction, T_e at increasing parameter ε above the bifurcation value ε_c. Notice that this extinction time diverges near the bifurcation value (results shown in a linear-linear plot). (b) Inverse square-root law also found in the system with no time lags (violet curve). Notice that the same power-law is found by including time lags. Here for all of the values of τ analyzed the time to extinction scales accordingly to $T_e \sim \psi^{-1/2}$.

equation (5) into $s = ce^s$, where $s = -(\lambda + kx_\pm)\tau$ and $c = -2\varepsilon\tau e^{kx_\pm\tau}$, whenever $0 < \varepsilon/k < 1/4$. Since $c < 0$ we conclude that the stability of $x_\pm$ is governed by a real eigenvalue such that x_+ is stable and x_- is unstable. In other words, the bifurcation at $\varepsilon/k = 1/4$ is also a saddle–node (s-n) bifurcation for the delayed model. The difference arises in how strong is the (un)stability at $(x_-)x_+$ depending on τ. When $0 < \varepsilon/k < 1/4$, it is quantified by the real number $\lambda = -kx_\pm - s/\tau$ being s the real solution of $c^2e^{2s} = s^2$, $s < 0$. After the bifurcation, i.e. $\varepsilon/k > 1/4$, the stability of $x_\pm$ is determined by the eigenvalue with maximum real part of Eq. (5). According to Theorem 1.2 in [30] $x_\pm$ are unstable regardless of the value of $\tau > 0$. ■

The dynamics near $x = 1/2$ after the s-n is slow, and it can be seen as a passage near a saddle equilibrium point (with complex coordinates). Hence, the time needed to "go through" $x = 1/2$ depends on the size of the real part of the eigenvalue of this saddle. To study the behaviour of the dominant eigenvalue when the points $x_\pm$ are complex, i.e. $\varepsilon/k > 1/4$, let us study Eq. (5) in a neighbourhood of $(x, \tau) = (1/2, 0)$. To this end, let us fix a small value $\delta > 0$ and let us write $\varepsilon/k = (1 + \delta)/4$. Then $x_\pm = (1 \pm \mathtt{i}\sqrt{\delta})/2$ are complex numbers and Eq. (5) becomes

$$1 \pm \mathtt{i}\sqrt{\delta} - (1 + \delta)e^{-\lambda\tau} + 2\lambda/k = 0. \tag{6}$$

As $(\tau, \lambda) = (0, 2\varepsilon - kx_\pm)$ verifies this equation and the derivative with respect to λ at this point is $2/k$ (which is always different from zero), the Implicit Function Theorem implies

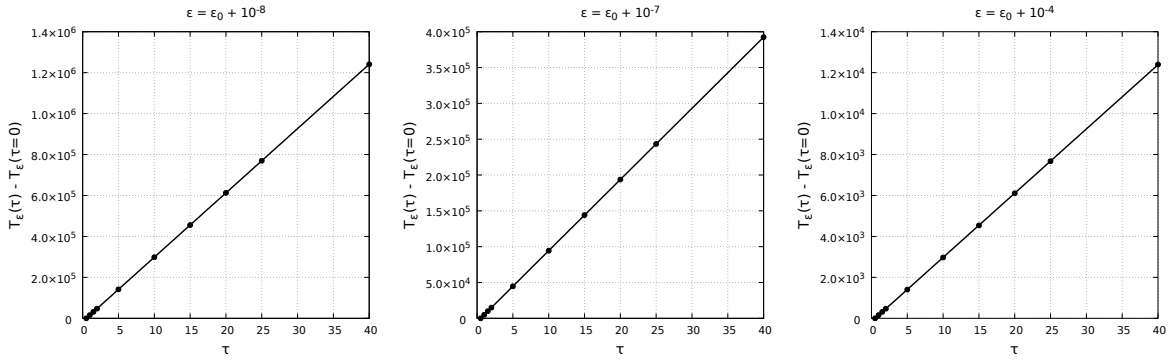

Figure 4: Linear dependence between the time that trajectories spend in the slow passage near the saddle-node remnant and the time lag τ. The points indicate the difference between the delayed transition for the system with no time lag and with different time lags, computed as $T_e(\tau) - T_e(\tau = 0)$, while the solid line is the linear regression. We display these results for three different values of the bifurcation parameter ε beyond the bifurcation value ε_c, plotting this difference between times at increasing lag times, τ.

the existence of a unique analytic mapping $\tau \mapsto \lambda(\tau)$ which verifies Eq. (6). It is tedious but not difficult to obtain that

$$\begin{aligned}\text{Re}\,\lambda(\delta,\tau) &= k\frac{\delta}{2} - k^2\left(\frac{\delta^2}{4}+\frac{\delta}{4}\right)\tau + k^3\left(\frac{3\delta^3}{2}+\frac{\delta^2}{2}+\frac{\delta}{8}\right)\frac{\tau^2}{2!} \\ &\quad -k^4\left(\delta^4+\frac{25\delta^3}{16}+\frac{3\delta^2}{8}-\frac{3\delta}{16}\right)\frac{\tau^3}{3!} \\ &\quad +k^5\left(\frac{125\delta^5}{32}+\frac{207\delta^4}{32}-\frac{\delta^3}{32}-\frac{131\delta^2}{32}-\frac{3\delta}{2}\right)\frac{\tau^4}{4!}+O(\tau^5).\end{aligned}$$

Proposition 2 $\text{Re}\,\lambda(\delta,\tau) = k\delta g(\delta,\tau)$ *for some analytic mapping* g *with* $g(0,0)\neq 0$.

Proof. It is enough to prove it in a neighborhood of $\delta = 0$. As the mapping $\lambda(\delta,\tau)$ is analytic, let us proceed by induction on the order of the derivative. Indeed, $\text{Re}\,\lambda(\delta,0) = k\delta/2$ and if now we assume that $\text{Re}\,\frac{\partial^i\lambda}{\partial\tau^i}(\delta,\tau)$ can be factorized by $k\delta$ for all $i<j$, then $\text{Re}\,\frac{\partial^j\lambda}{\partial\tau^j}(\delta,\tau)$ is the sum of a combination of $\text{Re}\,\frac{\partial^i\lambda}{\partial\tau^i}(\delta,\tau)$ with $i<j$ and the jth partial derivative of (6) with respect τ that always has $k\delta$ as a factor. ■

Table 1 shows the values of $\text{Re}\,\lambda(\delta,\tau)$ for different values of δ and τ, computed by solving numerically Eq. (6). Note the similarity between columns of this table, this is due to the form of $\text{Re}\,\lambda(\delta,\tau)$ (see Prop. 2). Moreover, as the derivative of $\text{Re}\,\lambda(\delta,\tau)$ at $\tau = 0$ is negative, we have that the real part of the eigenvalue becomes smaller as τ increases. Hence, we expect a longer transition time when a small delay is added.

By means of a numerical integration, we quantify the time that a trajectory is close to $x = 1/2$ for several values of τ. More concretely, we compute the time needed to go through $x = 1/2$ as the difference between the first time t that verifies $|\frac{dx}{dt}(t)| < 10^{-4}$ and $|x(t) - 1/2| < 0.005$ and the first one that does not verify it. Fig. 5 displays, in log scale,

τ	$\varepsilon_c + 10^{-4}$	$\varepsilon_c + 10^{-6}$	$\varepsilon_c + 10^{-8}$
0	2.000000e−04	2.000000e−06	2.000000e−08
0.05	1.950620e−04	1.950639e−06	1.950642e−08
0.1	1.902566e−04	1.902602e−06	1.902602e−08
1	1.259111e−04	1.259258e−06	1.259259e−08
1.5	1.037753e−04	1.037899e−06	1.037901e−08
2	8.748623e−05	8.749986e−07	8.750000e−09
5	4.255738e−05	4.256552e−07	4.256559e−09
10	2.175476e−05	2.175921e−07	2.175926e−09

Table 1: The greatest real part of eigenvalues of $x_\pm$ when $\varepsilon_c = 1/4$ and $k = 1$.

the relation between the values Re $\lambda(\delta, \tau)$ and the time taken to go through $x = 1/2$. Note that the plot shows the expected result for a linear system, in which the passage time near a saddle is proportional to the inverse of the largest real part of the eigenvalues of the saddle. As we are close to an equilibrium point, it is clear that the linear part dominates the dynamics and this implies a longer transition through $x = 1/2$.

Hence, this justifies the results displayed in Fig. 2 in the sense that τ involves a longer delayed transition near to the s-n remnant. In this figure three different values of ε are studied beyond, but close to the bifurcation. Specifically, we plot, for each case, a time series for the model given by Eq. (2) (violet trajectory $\tau = 0$), and six other trajectories applying increased time lags. For example, using $\varepsilon = \varepsilon_c + 10^{-8}$ the time delay with $\tau = 0$ is $t \approx 6 \times 10^3$, while for $\tau = 10$ this time becomes $t \approx 3.75 \times 10^5$. The dependence between the time delays and the distance to the bifurcation value for different time lags (including $\tau = 0$) is displayed in Fig. 3. Panel (a) displays the results in a linear-linear scale while (b) shows the same results in a log-log plot. Note that the time lag does not modify the inverse square-root law. Indeed, the increase of $\tau > 0$ in delaying times with respect to the model without time lags is linear. This relation is represented in Fig. 4, where the time differences for the model with $\tau = 0$ is plotted as a function of τ.

3 Discussion

Saddle-node (s-n) bifurcations arise in many nonlinear systems and can govern catastrophic transitions [1, 2, 8]. These bifurcations are typically found in systems with bistability, for which two different stable fixed points exist, and are separated by an unstable point in one dimension or by a separatrix in more than one dimension. Depending on the initial conditions, one of these two stable points will be achieved. Catastrophic transitions due to s-n bifurcations have been identified in mathematical models describing the dynamics of cooperation in biological systems [5, 16].

It is known that once the s-n bifurcation takes place, a s-n remnant (also called ghost) continues influencing the flows [11, 3]. That is, although the system becomes monostable after the s-n bifurcation, for extremely close values of the bifurcation parameter to the

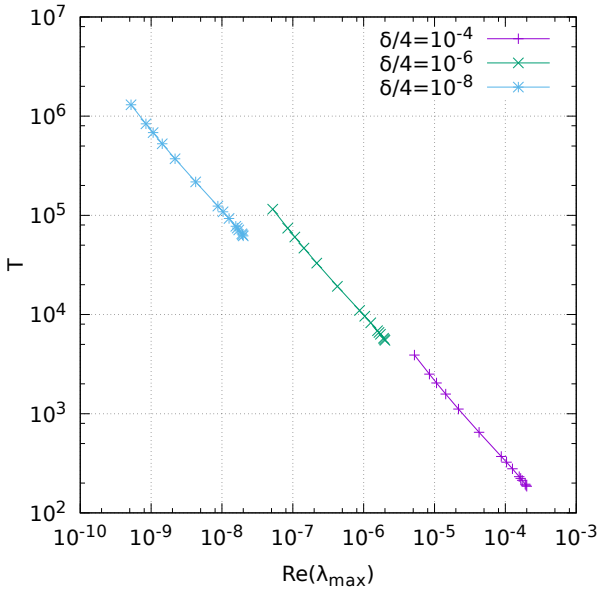

Figure 5: The values Re $\lambda(\delta, \tau)$ vs. the time spent near $x = 1/2$ for three values of δ: $\delta/4 = 10^{-4}$ (cyan), $\delta/4 = 10^{-6}$ (green), and $\delta/4 = 10^{-8}$ (violet).

bifurcation value, the flows experience a very long transient before reaching the single, asymptotically globally stable equilibrium. The times the system spends in this saddle remnant follow a power-law dependence that decays with exponent $-1/2$ as the bifurcation parameter increases near the bifurcation threshold. This exponent has been found in models with s-n bifurcations for charge density waves [11], electronic circuits (both theoretically and experimentally [12]), and nonlinear replicators [24, 7].

Despite the ubiquity of this phenomenon tied to s-n bifurcations, several questions still remain open. For instance, what is the impact of time lags in the dynamics near a s-n remnant. In this article we explore this question by using the simplest autocatalytic replicator model, which considers a single species or macromolecule that is able to catalyze itself. Our model assumes a logistic-like constraint in the growth of the population as well as density-independent decay. The dynamics of this model without time lags has been previously studied [7, 24].

We have found that the time lags, τ, further increase the length of the transients near the s-n remnant. Indeed, we have identified a linear increase of transients times at increasing time lags. Interestingly, the time lags do not modify the inverse square-root power law found in the s-n bifurcation [3, 7]. The model investigated here is the simplest one for models on autocatalysis of the form: $\dot{x} = kx(t-\tau_1)x(t-\tau_2)(1-x(t)/K) - \varepsilon x(t)$, where the interacting replicators experience different delays before being able to cooperate between each other. In this article we have considered the case $\tau_1 = \tau_2 = \tau$. More realistic models considering different lagged times (with $\tau_1 \neq \tau_2$) could be explored in the future. Indeed, the model investigated here can be extended to so-called hypercycle model [14]. Hypercycles are catalytic networks with cyclic architecture. This system, considering

delay differential equations, can be represented by the general model:

$$\frac{dx_i}{dt}(t) = k_{ij}x_i(t-\tau_i)x_j(t-\tau_j)\theta(\boldsymbol{x}(t)) - \varepsilon_i x_i(t),$$

with $\boldsymbol{x}(t) = \big(x_1(t), \ldots, x_n(t)\big)$, $x_i(t)$ being the population of the ith replicator at time t and n being the number of species forming the hypercycle (the hypercycle architecture involves $j = i-1$, with $j = n$ if $i = 1$). This model also considers a function $\theta(\boldsymbol{x}(t))$ introducing competition (e.g., a logistic function) and replicators' degradation proportional to ε_i.

Ghosts have been identified in symmetric and asymmetric two-member hypercycles [7, 15], in three- and four-member ones [17], as well as in high-dimensional hypercycles governed by periodic orbits [4, 5]. In [15] it was argued that delayed transitions in hypercycles might provide a selective advantage in fluctuating environments around bifurcation values, since a kind of memory could allow the recovery of hypercycles near bifurcation threshold [16]. The results of this manuscript reveal that lagging processes might actually enhance this memory effect.

Acknowledgements

The research leading to these results has received funding from 'la Caixa' Foundation. JG and AJ have been supported by the Spanish grants MTM2015-67724-P (MINECO/FEDER) and the Catalan grant 2014 SGR 1145. The project leading to this application has received funding from the European Union's Horizon 2020 research and innovation programe under the Marie Skłodowska-Curie grant agreement No 734557, and by a MINECO grant awarded to the Barcelona Graduate School of Mathematics under the "María de Maeztu" Program (grant MDM-2014-0445). JS has been also funded by a "Ramón y Cajal" Fellowship (RYC-2017-22243) and by the CERCA Programme of the Generalitat de Catalunya.

References

References

[1] M. Scheffer, S. Carpenter, J.A. Foley, C. Folke, and B. Walker. Catastrophic shifts in ecosystems. *Nature*, 413:591–596, 2001.

[2] M.G. Scheffer and S.R. Carpenter. Catastrophic regime shifts in ecosystems: linking theory to observation. *Trends Ecol. Evol.*, 18:648–656, 2003.

[3] S. H. Strogatz. *"Nonlinear Dynamics and Chaos with applications to Physics, Biology, Chemistry, and Engineering.* Westview Press, USA, 2000.

[4] D.A.M.M. Silvestre and J.F. Fontanari. The information capacity of hypercycles. *J. Theor. Biol.*, 254:804–806, 2008.

[5] A. Guillamon, E. Fontich, and J Sardanyés. Bifurcations analysis of oscillating hypercycles. *J. Theor. Biol.*, 387:23–30, 2015.

[6] S. Osborne, A. Amann, K. Buckley, G. Ryan, S.P. Hegarty, G. Huyet, and S. O'Brien. Antiphase dynamics in a multimode semiconductor laser with optical injection. *Phys. Rev. A*, 79:023834, 2009.

[7] J. Sardanyés and R. Solé. Bifurcations and phase transitions in spatially extended two-member hypercycles. *J. theor. Biol.*, 243:468–482, 2006.

[8] R. Solé. Scaling laws in the drier. *Nature*, 449:151–153, 2007.

[9] S.J. Schreiber. Allee effects, extinctions, and chaotic transients in simple population models. *Theor. Popul. Biol.*, 64:201–209, 2003.

[10] L. Dai, D. Vorselen, K.S. Korolev, and J. Gore. Generic indicators for loss of resilience before a tipping point leading to a population collapse. *Science*, 336:1175–7, 2012.

[11] S. H. Strogatz and R. M. Westervelt. Predicted power laws for delayed switching of charge density waves. *Phys. Rev. B*, 40(15):10501–10508, 1989.

[12] S. T. Trickey and L. N. Virgin. Bottlenecking phenomenon near saddle-node remnant in a Duffing oscillator. *Phys. Lett. A*, 248:185–190, 1998.

[13] M. Gomez, D.E. Moulton, and D. Vella. Critical slowing down in purely elastic 'snap-through' instabilities. *Nature Phys.*, 13:142–146, 2017.

[14] M. Eigen and P. Schuster. *The Hypercycle. A Principle of Natural Self-Organization.* Springer-Verlag, Berlin, 1979.

[15] J. Sardanyés and R. V. Solé. Ghosts in the origins of life? *Int. J. of Bif. and Chaos*, 16(9):2761–2765, 2006.

[16] J. Sardanyés and R. V. Solé. The role of cooperation and parasites in non-linear replicator delayed extinctions. *Chaos, Solitons and Fractals*, 31:1279–1296, 2007.

[17] J. Sardanyés and R. V. Solé. Delayed transitions in non-linear replicator networks: About ghosts and hypercycles. *Chaos, Solitons and Fractals*, 31:305–315, 2007.

[18] M. C. Mackey and L. Glass. Oscillations and chaos in physiological control systems. *Science*, 197:287–289, 1977.

[19] H. Barclay and P. van den Driessche. Time lags in ecological systems. *J. theor. Biol.*, 51:347–356, 1975.

[20] G. S. Ladde. Stability of model ecosystems with time-delay. *J. theor. Biol.*, 61:1–13, 1976.

[21] N. MacDonald. Time lag in a model of a biochemical reaction sequence with end product inhibition. *J. Theor. Biol.*, 67:549–556, 1977.

[22] M.R. Roussel. The use of delay differential equations in chemical kinetics. *J. Phys. Chem.*, 100:8323–8330, 1996.

[23] J.F.M. Avila and J.R.R. Leite. Time delays in the synchronization of chaotic coupled lasers with feedback. *OPTICS EXPRESS*, 17(24):21442–21451, 2009.

[24] E. Fontich and J. Sardanyés. General scaling law in the saddle-node bifurcation: a complex phase space study. *J. Phys. A: Math and Theor.*, 41:015102, 2007.

[25] A. Perachi. Origins of the temperature dependence of hammerhead ribozyme catalysis. *Nucleic Acids Res.*, 27(14):2875–2882, 1999.

[26] E.M. Barrrows. *"Animal behavior desk reference: a dictionary of animal behavior ecology, and evolution"*. (2nd Ed.) Boca Raton, Fla: CRC Press, 2001.

[27] P. Jarne and J.R. Auld. Animals mix it up too: the distribution of self-fertilization among hermaphroditic animals. *Evolution*, 60(9):1816–24, 2006.

[28] J. K. Hale and S. M. Verduyn Lunel. *Introduction to Functional Differential Equations*, volume 99 of *Applied Mathematical Sciences*. Springer New York, New York, NY, 1993.

[29] N. D. Hayes. Roots of the transcendental equation associated with a certain difference-differential equation. *Journal of the London Mathematical Society*, s1-25(3):226–232, 1950.

[30] J. Nishiguchi. On parameter dependence of exponential stability of equilibrium solutions in differential equations with a single constant delay. *Discrete and Continuous Dynamical Systems*, 36(10):5657–5679, 2016.

[31] R. Baltensperger, J.-P. Berrut, and B. Noël. Exponential convergence of a linear rational interpolant between transformed Chebyshev points. *Mathematics of Computation*, 68(227):1109–1121, 1999.

4 Appendix

Numerical tools

Numerical integration of the system with no time delays have been carried out using a $7th-8th$ order Runge-Kutta-Fehlberg method, with automatic step size control and local relative tolerance 10^{-15}.

In order to have an idea of how the numerical solution has been approximated numerically for the delay differential equation (DDE) model, let us explain some differences with respect to a standard ODE solver. The DDE in Eq. (4) can be expressed as

$$\frac{dx}{dt}(t) = f(x(t), x(t-\tau)),$$

with f being a suitable function. If the initial condition, which is necessary a continuous function, u is defined on the interval $[-\tau, 0]$. The Initial Value Problem can be shown as a chain of ODEs in each of the intervals $(l\tau, (l+1)\tau)$ where l denotes a positive integer. Therefore a natural integrator of these kind of DDE is just to consider a standard ODE solver and integrate in each of the different intervals. For instance, Let us consider a Runge-Kutta-Fehlberg (RKF) method. In order to approximate the next value it is needed to evaluate several times the function f, which involves to know values in the previous lag interval because of $x(t-\tau)$ term. Therefore the unknown previous values must be interpolated according to the previous information that one has been storing.
There are a lot of interpolation methods that allows us to approximate a value which is between the abscissae of a table of values. Let us formalize the one that was used in this paper. It is called *barycentric rational interpolation* [31]. Let $(s_i, \varphi_i)_{i=0}^n$ be a table of values of a scalar function φ defined in $[-1, 1]$. Let us assume that the abscissae take the values

$$s_i = \cos\left(\frac{i\pi}{n}\right), \qquad i = 0, \ldots, n.$$

Then the function

$$R_n[\varphi](s) = \frac{\dfrac{\varphi_0}{2(s-s_0)} + \displaystyle\sum_{i=1}^{n-1} \frac{(-1)^i \varphi_i}{s-s_i} + \frac{(-1)^n \varphi_n}{2(s-s_n)}}{\dfrac{1}{2(s-s_0)} + \displaystyle\sum_{i=1}^{n-1} \frac{(-1)^i}{s-s_i} + \frac{(-1)^n}{2(s-s_n)}},$$

is an interpolant of φ that does not have any pole in the interval $[-1, 1]$ and for analytic functions it converges exponentially. As a final comment, notice that one can consider the affinity $\phi\colon [-1, 1] \to [a, b]$ defined by $\phi(s) = \frac{1}{2}((a-b)s + a + b)$ and the interpolation does not depend on the interval $[-1, 1]$.

In our numerical results we have used a RK78F with barycentric rational interpolation.